RESEARCH ARTICLE

JOR *Spine* OPEN ACCESS

Collagen integrity of the annulus fibrosus in degenerative disc disease individuals quantified with collagen hybridizing peptide

Manmeet S. Dhiman [1,2] | Taylor J. Bader [2,3] | Dragana Ponjevic [2,4] |
Paul T. Salo [2,5] | David A. Hart [2,5,6] | Ganesh Swamy [2,5] | John R. Matyas [2,4] |
Neil A. Duncan [2,7]

[1]Department of Biomedical Engineering, University of Calgary, Calgary, Alberta, Canada

[2]McCaig Institute for Bone and Joint Health, University of Calgary, Calgary, Alberta, Canada

[3]Department of Medical Sciences, University of Calgary, Calgary, Alberta, Canada

[4]Faculty of Veterinary Medicine, University of Calgary, Calgary, Alberta, Canada

[5]Department of Surgery, Cumming School of Medicine, University of Calgary, Calgary, Alberta, Canada

[6]Faculty of Kinesiology, University of Calgary, Calgary, Alberta, Canada

[7]Department of Civil Engineering, University of Calgary, Calgary, Alberta, Canada

Correspondence
Neil A. Duncan, McCaig Institute for Bone and Joint Health, University of Calgary, Calgary, Alberta, Canada.
Email: duncan@ucalgary.ca

Abstract

Introduction: Degenerative disc disease (DDD) is accompanied by structural changes in the intervertebral discs (IVD). Extra-cellular matrix degradation of the annulus fibrosus (AF) has been linked with degeneration of the IVD. Collagen is a vital component of the IVD. Collagen hybridizing peptide (CHP) is an engineered protein that binds to degraded collagen, which we used to quantify collagen damage in AF. This method was used to compare AF samples obtained from donors with no DDD to AF samples from patients undergoing surgery for symptomatic DDD.

Methods: Fresh AF tissue was embedded in an optimal cutting temperature compound and cryosectioned at a thickness of 8 μm. Hematoxylin and Eosin staining was performed on sections for general histomorphological assessment. Serial sections were stained with Cy3-conjugated CHP and the mean fluorescence intensity and areal fraction of Cy3-positive staining were averaged for three regions of interest (ROI) on each CHP-stained section.

Results: Increases in mean fluorescence intensity ($p = 0.0004$) and percentage of positively stained area ($p = 0.00008$) with CHP were detected in DDD samples compared to the non-DDD samples. Significant correlations were observed between mean fluorescence intensity and percentage of positively stained area for both non-DDD ($R = 0.98$, $p = 5E-8$) and DDD ($R = 0.79$, $p = 0.0012$) samples. No significant differences were detected between sex and the lumbar disc level subgroups of the non-DDD and DDD groups. Only tissue pathology (non-DDD versus DDD)

influenced the measured parameters. No three-way interactions between tissue pathology, sex, and lumbar disc level were observed.

Discussion and Conclusions: These findings suggest that AF collagen degradation is greater in DDD samples compared to non-DDD samples, as evidenced by the increased CHP staining. Strong positive correlations between the two measured parameters suggest that when collagen degradation occurs, it is detected by this technique and is widespread throughout the tissue. This study provides new insights into the structural alterations associated with collagen degradation in the AF that occur during DDD.

1 | INTRODUCTION

Low back pain (LBP) is the world's leading cause of years lived with disability, affecting at least 619 million people globally in 2020.[1] LBP has been strongly linked with degenerative disc disease (DDD), but a full understanding of the role of collagen integrity of the intervertebral disc (IVD) during the pathogenesis of disc degeneration remains obscure.[2–5] DDD is marked by both mechanical and biochemical changes in the intervertebral discs (IVD).[6] At the time of surgery for symptomatic DDD, the IVDs of affected individuals often exhibit severe destructive changes in annulus fibrosus (AF) tissue with tears and delamination of the collagenous lamellae, suggesting that the degradative process is rather prolonged. These observations suggest degradation of the AF, and that collagen damage may be a key pathological and therapeutic target in DDD.

The IVD undergoes continuous modeling and remodeling throughout human growth and aging, with a healthy proposed balance between catabolism and anabolism of the extracellular matrix (ECM).[7,8] However, in DDD, ECM catabolism outpaces anabolism and results in the degeneration of the IVD.[8] Even so, quantifying the ECM degradation has been challenging.[9] Collagen is a vital part of the ECM, comprising approximately 70% of the dry weight in the IVD, and it is the protein that provides the disc with its remarkable resistance to tensile loads.[10,11] The biosynthesis of collagen requires the winding of three propeptide chains into a triple helix to form mature fibrillar collagen, which is very stable at body temperatures and only denatures when cleaved by specific proteases.[12,13] Historically, degraded collagen has been difficult to quantify. While some studies have attempted to quantify the degeneration in the IVD using second-harmonic generation (SHG) imaging, but this method does not directly quantify collagen degradation and integrity.[14–17] Collagen integrity is defined as its ability to provide appropriate support to the ECM and the disc structures to maintain homeostasis and proper functioning. Other studies have attempted to study collagen degradation in DDD using histology or immunohistochemistry,[18–20] but these approaches are also ill-suited to specifically quantify collagen damage. For example,

histochemical dyes bind to all types of collagen molecules regardless of the damage or collagen subtype.[18,19] While anti-collagen antibodies are very specific, the use of such antibodies to detect collagens in histological sections is plagued by non-specific background staining and the inability to distinguish between intact, damaged, and denatured collagen.[20]

Recently, a Collagen Hybridizing Peptide (CHP) has been reported as being able to identify and quantify collagen damage in IVDs and other connective tissues at the molecular level.[9,14,21–25] Briefly, CHP binds selectively to the dissociated triple helix structure in the degraded collagens through a unique helix hybridization process,[12,21] mimicking the triple-helical molecular structure of natural collagen, where it binds to the glycine (G)-proline (P)-hydroxyproline (O) amino acid repeat chains in the fibrillar triple helical domain.[12] Through hydrogen bonding, a stable homotrimeric triple helix is formed. Previously, Weiss and colleagues reported that CHP has negligible affinity for intact collagen due to a lack of binding sites and negligible non-specific binding due to its neutral and hydrophilic sequence.[21] These authors also demonstrated that CHP with intact chains had no binding affinity towards denatured chains of native collagen.[21] Various studies have shown that CHP can bind to collagens degraded by various processes, including enzymatic digestion, heat, or mechanical injury.[12,13,21,26] This method allows for more accurate relative intensity and spatial quantification of collagen damage due to its specificity compared to histology or immunohistochemistry. The CHP signal is visualized using fluorescence microscopy at different wavelengths, with a variety of fluorophores.[9,21,23]

Weiss and colleagues used CHP to quantify collagen damage in Sprague Dawley rat tail tendon fascicles.[21] To our knowledge, this study was the first to use CHP for monitoring connective tissue disease and injury. Their study showed that collagen denaturation was associated with the onset of mechanical damage. To date, only a few studies have examined the use of CHP to detect collagen damage in the AF,[9,14,23,25] of which only two use human AF.[9,23] However, the focus of those studies was on various murine models whereas human samples were not examined in detail. Liu and colleagues examined

murine models with age-related degenerated and mechanical injury.[23] In both cases, the fluorescence intensity of CHP increased with age and injury. Human samples of degenerated AF had increased CHP intensity correlating with increasing Pfirrmann Grade. Xiao and colleagues treated murine discs with IL-1β and lipopolysaccharide (LPS) to induce matrix degradation, by upregulation of MMPs and subsequent collagen cleavage.[9] Both treatment groups (e.g., IL-1β and LPS) displayed increased collagen denaturation and CHP intensity compared to the control groups. They also reported that degenerated human IVD samples had increased CHP fluorescence intensity compared to non-DDD human IVD samples.[9,23]

There is evidence that sex and lumbar disc level may also play a role in the development of DDD. As the prevalence of DDD is increased in females compared to males,[27–30] and as there could be differing responses to injury between the two sexes,[17,31] it becomes relevant to analyze the findings based on sex. Additionally, previous studies have usually examined samples from a single lumbar level or combined samples from various lumbar levels.[9,14,23,25] However, the different lumbar levels operate in a distinct and unique mechanical environment,[32,33] degenerating at different rates,[34] thus suggesting further study of structural differences of different lumbar levels.

We hypothesized that using CHP and AF samples from surgical DDD individuals would lead to increasing binding of the reagent, consistent with decreased structural integrity of the tissue compared to non-diseased controls. Furthermore, we hypothesized that such changes would be influenced by the sex and lumbar disc level. The purpose of the study was to quantify the mean fluorescence intensity and areal fraction of CHP staining in a region of interest (ROI) of fresh AF samples from surgical DDD individuals and non-DDD organ donors. We used standard Hematoxylin and Eosin (H&E) staining imaging and polarized light microscopy imaging to compare CHP to alternative methods of structural imaging.

2 | METHODS

2.1 | Inclusion/exclusion criteria and ethics

Fresh human AF samples were obtained after removal from individuals undergoing anterior lumbar surgery for DDD at L4-L5 and L5-S1 levels (based on the superior-anterior landmark noted by surgeons). Non-DDD fresh samples were obtained within 1–2 h of death from younger organ donors through the Southern Alberta Tissue Donation program after organ harvest completion. All samples were obtained with local ethics approval (University of Calgary Ethics ID: REB18-1308).

2.2 | Demographics

Age, body mass index (B.M.I.), and sex distribution are reported by the number of individuals whereas the Pfirrmann Grade and Level distribution are reported by the number of samples (Table 1). B.M.I. and

TABLE 1 Demographic information of the non-DDD and DDD individuals included in the present study.

	Non-DDD	DDD
Number of individuals	6	13
Number of samples	12	14
Age (years)*	34 ± 10	45 ± 10
B.M.I.	N/A	27.3 ± 3.0
Pfirrmann grade	N/A	6.8 ± 1.1
Radiographic degeneration grade	0.25 ± 0.45	N/A
Sex (M/F)	(4/2)	(8/5)
Level (L4-L5/L5-S1)	(6/6)	(5/9)

*$p \leq 0.05$ for the parameter comparison.

Pfirrmann Grade were not available for the non-DDD donors. Samples from spine deformities such as degenerative scoliosis and spondylolisthesis were not included. The radiographic grading system by Wilke et al.[35] was used to grade non-DDD samples (Table 1). However, preoperative CT scans were not available for most DDD individuals, so the modified Pfirrmann Grade by Griffith et al.[36] based on MRI imaging was used for DDD samples. CT scans did not show any significant amount of disc height loss for the non-DDD individuals (Figure S1).

2.3 | Tissue preparation

Fresh tissue with minimum dimensions of 2 mm × 2 mm × 2 mm (circumferential length × tissue width [disc height] × radial length) was obtained from surgery and embedded immediately in the optimal cutting temperature (OCT) compound within 30 min of tissue resection from the individual and stored at −80°C until cryosectioning (Figure 1). The tissue was sectioned in the axial/transverse plane at 8 μm thickness at −20°C in the cryostat. Sequential tissue sections (2–3 sections per sample/slide) of the tissue were mounted on Superfrost Plus Micro Slides (VWR, Pennsylvania), incubated overnight at 37°C, and stored at −20°C until the staining procedures. Slides were carefully examined under a microscope to determine the gross quality of sections and those with the fewest cutting artifacts were selected for further histological (H&E), CHP, and LC-PolScope analysis. LC-PolScope sections were mounted unstained.

2.4 | Hematoxylin and Eosin (H&E) staining and scoring

Standard H&E staining protocols were followed, and details can be found in the Supporting Information Section S1. All slides were scanned with the Zeiss Axio Scan.Z1 Scanner (Zeiss Group, Germany) at 10× Brightfield imaging with flash intensity of 249% and flash duration of 4 μs.

Three knowledgeable researchers graded the AF sections stained with H&E in an independent and blinded manner for histological degeneration grading based on the criteria outlined by Le Maitre and

Posterior
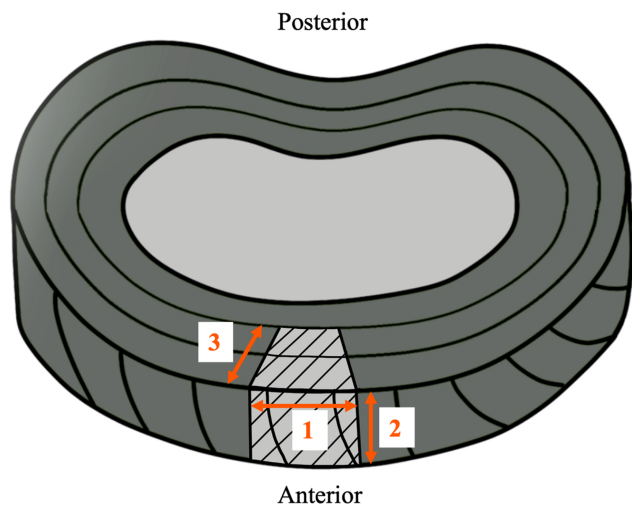
1. Circumferential Length

2. Tissue Width/Disc Height

3. Radial Length

Anterior

FIGURE 1 Schematic of the intervertebral disc showing the location of the AF samples utilized in the study from the DDD individuals and non-DDD donors. Sample dimensions (minimum 2 mm × 2 mm × 2 mm) are labeled as (1) circumferential length, (2) disc height/tissue width, and (3) radial length.

colleagues.[37] The current histological sections only had the AF with no interface between the nucleus pulposus (NP), endplates, and the AF. Thus, the criteria were modified to remove interface zone assessments.

2.5 | Collagen hybridizing peptide (CHP) staining

Initial studies were performed to optimize the CHP staining protocol (see Supporting Information Sections S2 and S3). Each slide underwent washing in distilled water (dH$_2$O) and 2 × 1XPBS (Phosphate Buffered Saline) for 5 min each to remove the OCT compound. Thirty microliters of 1XPBS with 1% BSA (Bovine Serum Albumin) and 5% goat serum was applied on each section for non-specific blocking and the slide underwent incubation at room temperature for 1 h. The CHP was pre-conjugated with the Cy3 fluorophore (Advanced Biomatrix, Catalogue Number: 5276-60UG). The stock CHP solution (100 μM) at 4°C was diluted to 1 μM (1:100 dilution), heated to 85°C for 5 min, and immediately quenched in an ice bath for 1 min. CHP solution (25 μL) was applied immediately onto each section to achieve minimal dead time. The slides were incubated at 4°C for 4 h. After incubation, the slides were dynamically washed 4 times for 15 min each in 1XPBS solution. Next, 30 μL of anti-fade hard-set mounting media with DAPI (Biotium, California, Catalogue Number: 23004) was applied to each section and covered with a coverslip. The slides were incubated overnight at 4°C. All slides were then scanned with a Zeiss Axio Scan.Z1 Scanner (Zeiss Group, Germany) at 10× fluorescence imaging with light source intensity of 80% and exposure duration of 150 ms. The Cy3 fluorophore was detected at 563 nm wavelength.

2.6 | Quantification of the CHP signal

Three Regions of Interest (ROIs) (900 μm squares) were chosen for one section per slide while ensuring there were no folds and artifacts in the ROI. If the sample had high fluorescence heterogeneity, then ROIs were chosen to reflect the heterogeneity in the calculations. The size of the ROI was chosen such that three representative ROIs could be selected from most samples. On the Zen software (Version 3.5, Zeiss Group, Germany), a small threshold was applied on the 16-bit ROI images to accurately segment the positively stained foreground from the non-tissue surrounding background. Consequently, the pixel intensities associated with the background were removed and only the fluorescence intensity of the positive staining (foreground) was quantified. Thresholding was performed because of minor differences in the available background in each ROI and to remove the impact of background on quantification of positive staining. To minimize the bias in removing the background during thresholding, a sensitivity analysis was performed (see Supporting Information Section S4 for the rationale on the use of thresholding) to compare the threshold and non-threshold approaches. The fluorescence intensity of the fluorophore, Cy3, was quantified in the Zen software (Version 3.5, Zeiss Group, Germany) using the fluorescence intensity of the Cy3 channel calculated in the ROI. The ROIs used for fluorescence intensity quantification were used for the calculations of percentage of area in the ROI stained positively. Images from the channel were imported into ImageJ[38] and converted to an 8-bit grayscale image. Based on the previously established thresholds for mean fluorescence intensity to determine the positive staining of CHP in the ROI, the amount of positively stained area was recorded as a percentage of the total ROI area.

2.7 | Polarimetry

Unstained 8 μm sections were mounted and imaged using circularly polarized light at 546 nm wavelength (LC-PolScope CRI, Boston) on a light microscope (Axioplan2, Carl Zeiss Microscopy, USA) at 5× magnification with maximum retardance of 60 nm. The same ROIs used for CHP analysis were used for LC-PolScope imaging. A retardance/azimuth composite image and an azimuth histogram was obtained for each ROI. Retardance is the phase shift between the light traveling

through the fast and slow axis of the birefringent collagen fibers with different refractive indices. Azimuth is the orientation/angle of the birefringent collagen fibers ranging from 0° to 180°. The range of the peak(s) in the azimuth histogram for each ROI was recorded as a measure of disorganization of collagen fibers (modified from Mountain et al.[39] and Al-Saffar et al.[40]).

2.8 | Statistics

Shapiro–Wilk normality tests and F-tests were performed to check for normality and differences between variances of the groups before conducting statistical significance tests. Because of the directionality of the hypothesis based on previous literature, one-tailed Student's t-tests, Welch t-tests, and Mann–Whitney U-tests were performed to test for significance of differences between samples from different groups (Non-DDD vs. DDD, male vs. female, and L4-L5 vs. L5-S1) for mean fluorescence intensity and percent positive ROI area. Pearson and Spearman correlations were performed between the mean fluorescence intensity and percent positive ROI area, and with respect to age and histological degeneration score. Three-way Analysis of Variance (ANOVA) measures were performed to examine the interaction effects between the following three factors: Tissue Pathology, Sex, Lumbar Disc Level. Bonferroni corrections were applied to the ANOVA interaction p-values. The type I error was set to $\alpha = 0.05$. More details can be found in Supporting Information Section S6.

3 | RESULTS

3.1 | Histological degeneration grade and aging

High inter-rater variability was observed for histological degeneration scoring ($\kappa = 0.0048$) (Figure 2). However, the differences between non-DDD and DDD samples were consistent for each reviewer with the average difference being 2.78 ± 0.56. Samples from DDD individuals had an elevated histological degeneration score compared to the samples from non-DDD individuals (5.95 ± 1.94 vs. 3.17 ± 1.04, $p = 0.00007$) (Figure 2). The histological score of DDD samples had a weak correlation with the average mean fluorescence intensity (Spearman coefficient $R = 0.26$) whereas no correlation was observed with the average percentage of positively stained ROI area (Spearman coefficient $R = -0.08$). The histological scores for non-DDD samples did not show any correlations with the average mean fluorescence intensity (Spearman coefficient $R = 0.05$) and the average percentage of positively stained ROI area (Spearman coefficient $R = 0.12$). Histological degeneration scores were increased for DDD females compared to DDD males (7.33 ± 1.72 vs. 5.18 ± 1.68, $p = 0.04$) whereas they were not different for non-DDD females and males (Table 2).

Age was negatively correlated with both the average mean fluorescence intensity (Pearson coefficient $R = -0.65$) and the average percentage of positively stained area in the ROI (Pearson coefficient $R = -0.62$) for the non-DDD samples. However, age was positively correlated with the average mean fluorescence intensity (Spearman coefficient $R = 0.63$) and the average percentage of positively stained area in the ROI (Pearson coefficient = 0.56) for the DDD samples. No differences were found between the ages of males and females across both non-DDD and DDD groups (Table 2).

3.2 | Tissue pathology comparison using CHP staining and LC-PolScope

H&E staining qualitatively showed greater structural defects such as AF fissures/tears and reduced lamellar organization in the DDD samples compared to the non-DDD samples (Figure 3). Tissue obtained from DDD individuals had an increased average mean fluorescence intensity ($p = 0.0004$) and average percent positive ROI area ($p = 0.00008$) compared to the samples obtained from the non-DDD donors (Figure 3). The average mean fluorescence intensity (arbitrary units [a.u.]) was 10103 ± 3370 for DDD samples and 6301 ± 1654 for non-DDD samples. The average percent positive area per ROI was 46.5 ± 18.9% for DDD samples and 18.8 ± 11.0% for non-DDD samples (Figure 3). Qualitatively, DDD samples exhibited more intense local binding of CHP combined with the spatial binding across the entire tissue section as compared to the non-DDD samples. Tissue from DDD individuals exhibited an increased azimuth range for the collagen fibers compared to the samples from non-DDD individuals (104.8 ± 20.1° vs. 69.3 ± 20.1°, $p = 0.00008$) (Figure 4).

3.3 | Linear regressions of the parameters

The average mean fluorescence intensity and average percent positive area per ROI were significantly correlated in both non-DDD (Pearson coefficient $R = 0.98$, $p = 5.0E-8$) and DDD individuals (Spearman coefficient $R = 0.79$, $p = 0.001$) (Figure 5).

3.4 | Sex

No statistical differences were observed between tissue from male and female DDD individuals for average mean fluorescence intensity (a.u.) (9647 ± 3878 vs. 10 922 ± 2351) and average percent positive ROI area (45.5 ± 21.6% vs. 48.3 ± 14.9%) (Figure 6). However, in non-DDD male donors, there was a trend towards increased average mean fluorescence intensity (6814 ± 1783 vs. 5273 ± 702) ($p = 0.067$) and increased average percent positive area per ROI (22.1 ± 12.2% vs. 12.2 ± 3.6%) ($p = 0.076$) compared to non-DDD female donors (Figure 6).

3.5 | Lumbar disc level

No differences (although modest trends were detected) were observed between tissue from DDD L4-L5 and L5-S1 samples for average mean fluorescence intensity (a.u.) (8865 ± 1792 vs. 10 790
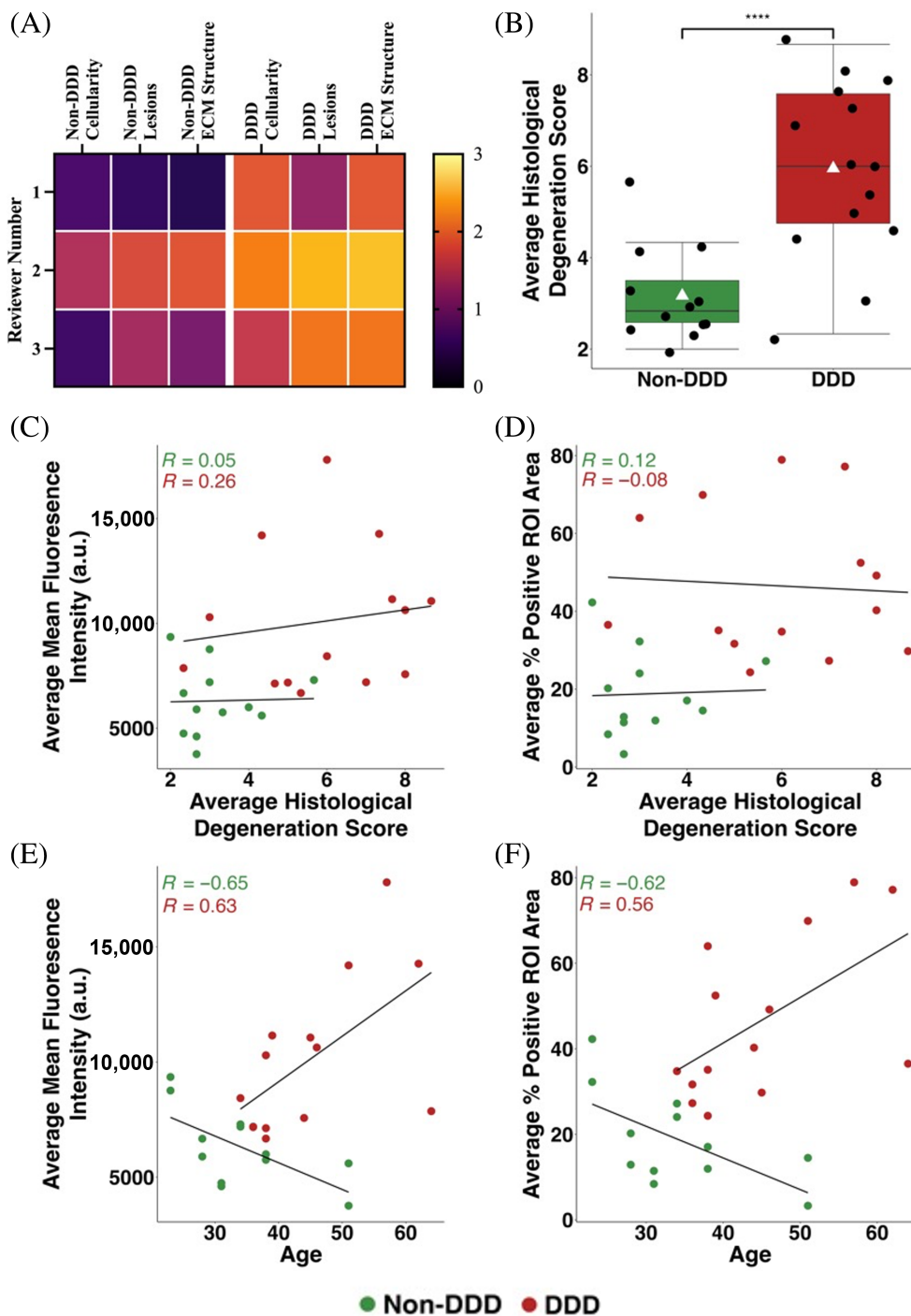
FIGURE 2 Histological degeneration scoring was performed by three independent and blinded spine researchers. (A) The heat map outlines the scores of each reviewer for each scoring category for non-DDD and DDD samples. (B) Scores were averaged across reviewers and a comparison between non-DDD and DDD samples was performed. **** represents $p \leq 0.0001$. Linear regression correlations of the average mean fluorescence intensity (a.u.) and average ROI area stained positively with CHP with respect to histological degeneration grade (C & D) and age (E & F) of the included individuals were performed. Spearman correlations were performed for the histological degeneration score. For age, (E) shows the Pearson correlation for the non-DDD samples and the Spearman correlation for the DDD samples whereas (F) shows Pearson correlations for both the non-DDD and DDD samples.

TABLE 2 Age and histological degeneration score for non-DDD and DDD males and females.

	Non-DDD		DDD	
	Male	Female	Male	Female
Age (years)	34 ± 12	35 ± 5	46 ± 13	45 ± 4
Histological Degeneration grade	3.21 ± 1.21	3.08 ± 0.74	5.18 ± 1.68*	7.33 ± 1.72

*A statistically significant difference between DDD males and females for the histological degeneration score ($p \leq 0.05$).

± 3919) ($p = 0.16$) and average percent positive area per ROI (37.9 ± 15.3% vs. 51.3 ± 19.8%) ($p = 0.11$) (Figure 7). Furthermore, no differences were observed between non-DDD L4-L5 and L5-S1 samples

for average mean fluorescence intensity (6358 ± 1460 vs. 6244 ± 1969) and average percent positive ROI area (19.2 ± 8.5% vs. 18.4 ± 14.0%) (Figure 7).
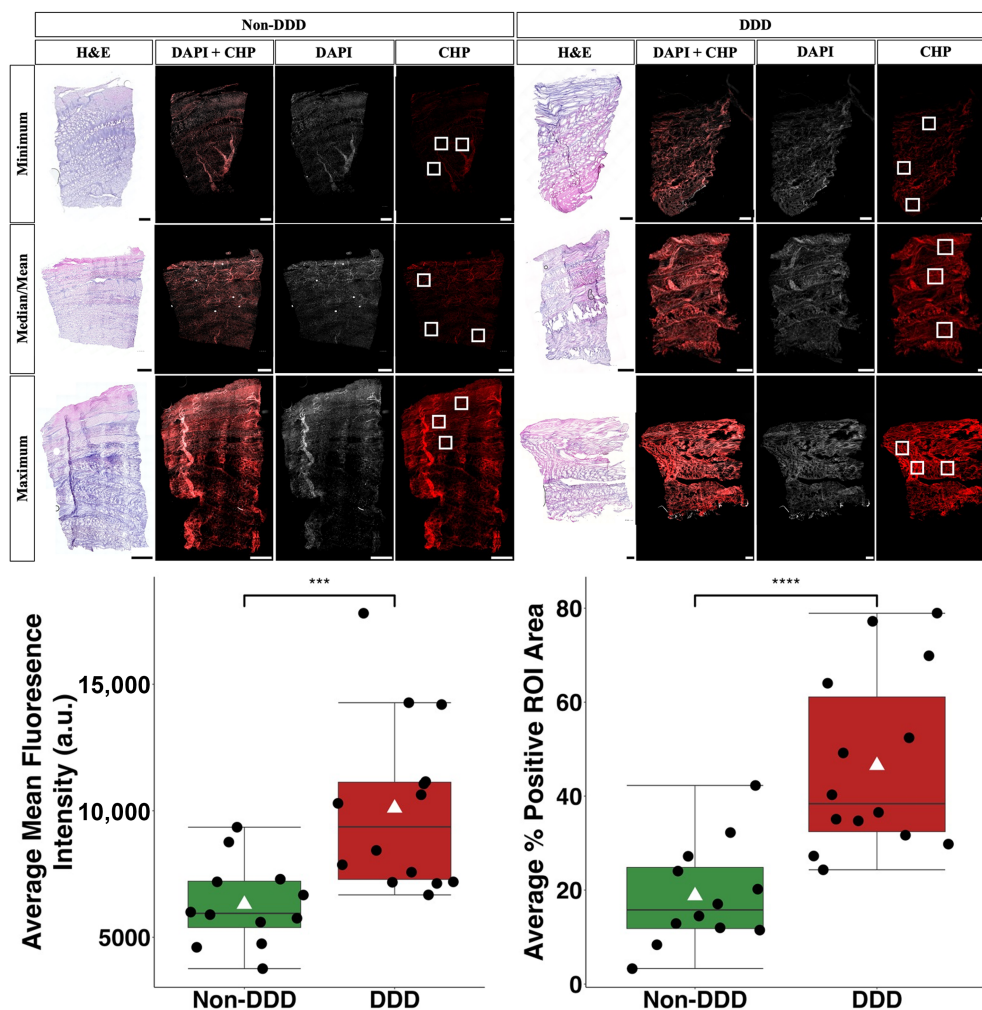
FIGURE 3   Non-DDD and DDD AF sample sections in the axial/transverse plane represent the minimum, median/mean, and maximum average mean fluorescence intensity within the group using DAPI + CHP, DAPI, and CHP channels. The red color in the CHP channel depicts positive staining (excluding the artifact staining). Three white boxes in the CHP image show the ROIs chosen to calculate the average mean fluorescence intensity and average percentage of positively stained ROI area. Qualitative morphological comparison is shown with hematoxylin & eosin (H&E) staining. The top of the image is the anterior outer AF and the bottom of the image is closer to the inner AF of the sample. For non-DDD samples, scale bar = 1000 μm and for DDD samples, scale bar = 500 μm. Average mean fluorescence intensity (a.u.) and average positive CHP staining as a percentage of the total ROI area are compared between non-DDD and DDD samples. The horizontal line in the middle of the boxplot represents the median and the white triangle represents the mean of the group. **** represents $p \leq 0.0001$ and *** represents $p \leq 0.001$.

3.6 | Interaction effects

Only the tissue pathology (non-DDD and DDD) influenced both average mean fluorescence intensity ($p = 0.004$) and average percent positive area per ROI ($p = 0.0005$) (Table 3). Neither sex nor lumbar disc level influenced either property. No two-way or three-way interactions were observed between tissue pathology, sex, and lumbar disc level.

4 | DISCUSSION

Degenerated surgical AF samples exhibited increased average mean fluorescence intensity and average percent positive ROI area compared to non-DDD samples. The main finding of the current study is the decreased collagen integrity, as visualized by elevated CHP staining, in the DDD samples compared to tissue samples from non-DDD donors. Previous studies showed increased CHP labelling in degenerated human and animal samples compared to non-degenerated samples.[9,23] To the best of our knowledge, this is the first study to perform a rigorous analysis of relative changes of collagen integrity in non-DDD and DDD human AF tissue. The relative fluorescence intensity changes between the non-degenerated and degenerated disc of the current results were similar in magnitude (1.7 times greater signal in the degenerated samples compared to the non-degenerated samples) to that reported by Xiao et al.[9] Liu et al. reported a linear increase in fluorescence intensity with respect to increasing Pfirrmann Grade in human samples (Grade II–V on the
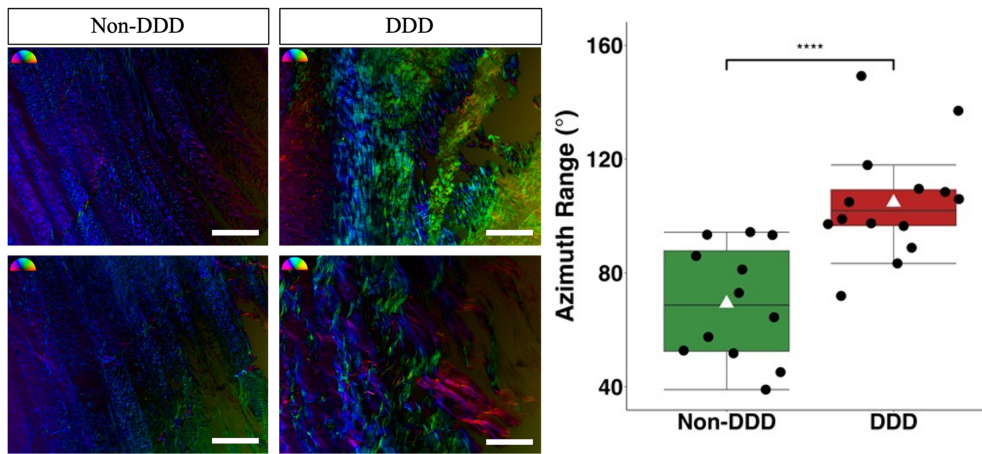
FIGURE 4 Two non-DDD and DDD sample region of interests (ROI) in the transverse plane to represent the retardance and azimuth composite image for the collagen fibers. The intensity of color represents the retardance value (higher intensity = higher retardance) and the location of the color on the color wheel in the top left corner of the images represents the azimuth. The right side of the color wheel represents 0° whereas the left side represents 180°. Azimuth range across the ROI is calculated from the azimuth histograms and is compared between non-DDD and DDD samples. The white triangle represents the mean of the respective group. **** represents $p \leq 0.0001$. Scale Bar = 500 μm.
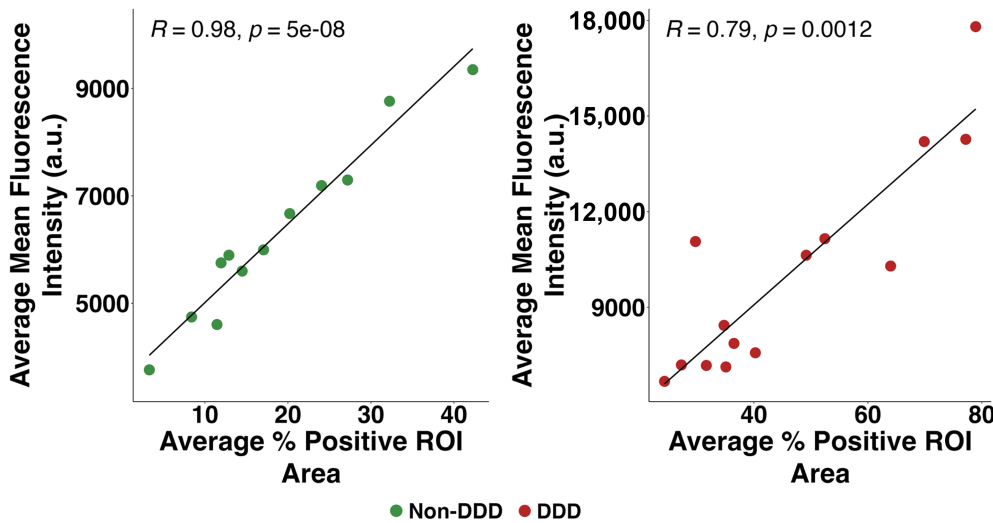
FIGURE 5 Linear regression correlations of the average mean fluorescence intensity (a.u.) and average ROI area stained positively with CHP. The left graph shows the Pearson correlation among non-DDD samples whereas the right graph shows the Spearman correlation among DDD samples.
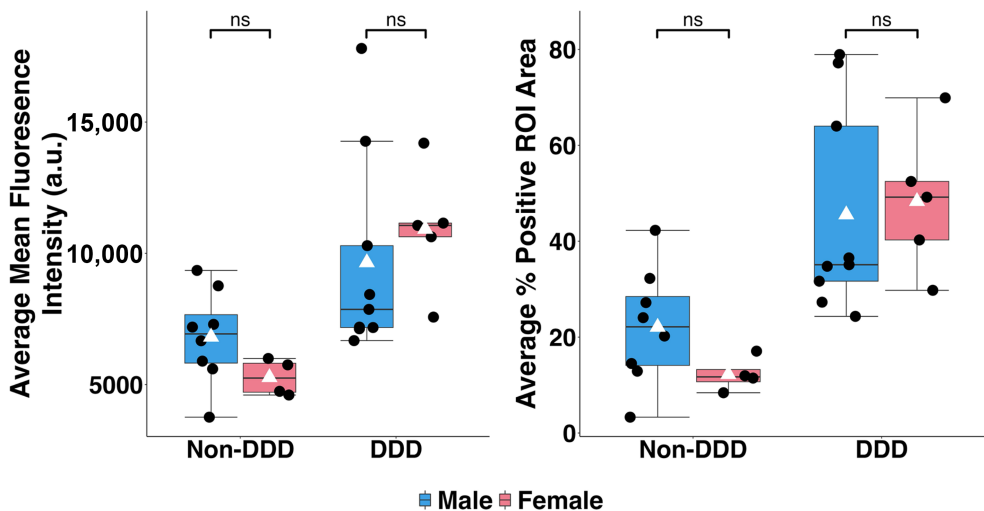

FIGURE 6 The average mean fluorescence intensity (a.u.) and average positive CHP staining as a percentage of the total ROI area are compared between male and female human IVD AF samples of the non-DDD and DDD groups. The horizontal line in the middle of the boxplot represents the median and the white triangle represents the mean of the group. ns represents $p \geq 0.05$.
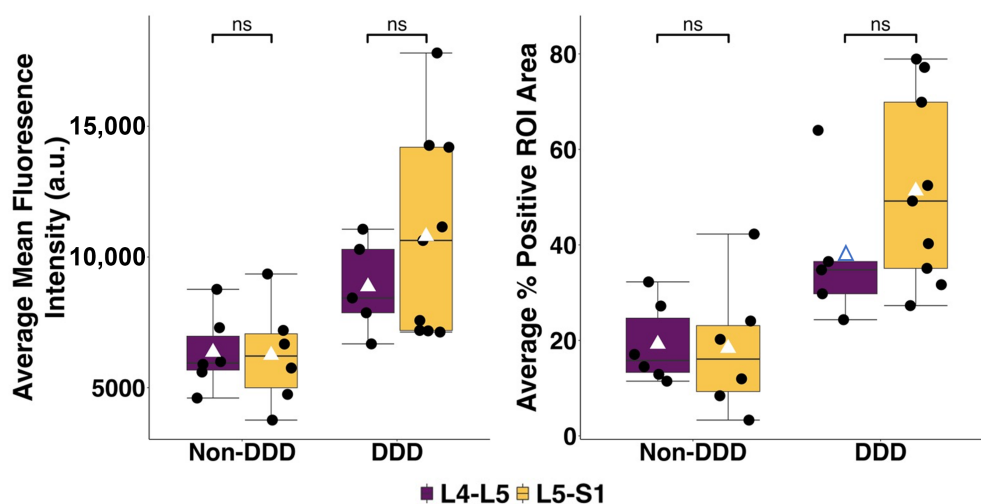
FIGURE 7 The average mean fluorescence Intensity (a.u.) and average positive CHP staining as a percentage of the total ROI area are compared between L4-L5 and L5-S1 human IVD AF samples of the non-DDD and DDD groups. The horizontal line in the middle of the boxplot represents the median and the white triangle represents the mean of the group. ns represents $p \geq 0.05$.

TABLE 3 ANOVA three-way interaction effects for adjusted p-values with the factors of condition, sex, and level for the comparison of average mean fluorescence intensity and average percent positive ROI area.

	Average mean Fluorescence intensity	Average percent Positive ROI area
Tissue pathology	0.004	0.0005
Sex	0.99	0.67
Lumbar level	0.43	0.31
Tissue pathology: sex	1	1
Tissue pathology: lumbar level	1	1
Sex: lumbar level	1	1
Tissue pathology: sex: lumbar level	1	1

Note: Bonferroni corrections have been applied for multiple comparisons.

original scale).[23] However, their human samples were from a variety of IVD degeneration models including herniated discs whereas the present study only examined DDD. Percent positive area of the ROI was not measured in any previous studies.

Surgical DDD samples further exhibited increased range of the azimuth compared to the non-DDD samples. This suggests that the collagen fibers are orientated across a wide range of angles, indicating increased randomness in their organization in the DDD samples. The smaller range for non-DDD samples indicates greater uniformity in their organization. Annular disorganization has been previously linked to degeneration of the IVD due to age[41] and DDD.[42] Furthermore, collagen disorganization has been associated with IVD degeneration.[43] However, disorganization is not necessarily congruent with degeneration of the collagen fibers. Further studies will be required to determine the association between the disorganization of the collagen fibers, the structural integrity of collagen, and the degeneration of the AF.

Adams and Roughley have reported that the IVD undergoes structural modifications including annulus tears (circumferential tears, peripheral tears, and radial fissures).[7] Since the main structural component of the AF is collagen, specifically the fibrillar collagen type I in the outer AF,[11] the current studies provide further evidence that degenerated discs exhibited structural alterations consistent with decreased collagen integrity compared to non-DDD discs. Various soft tissues such as cartilage, bone, skin, and the IVD have been shown to undergo collagen remodeling in different pathological states.[11,44–48] In the current study, the effect of collagen turnover rate and the dysregulation of normal collagen turnover with respect to collagen degradation was not explored. Sivan and colleagues determined that the collagen turnover rate for degenerated IVDs was greater compared to non-DDD IVDs where the collagen turnover is more regulated.[11,48] Increased dysregulated collagen turnover rate would lead to increased binding of the CHP to the GPO sequences, thus being consistent with overt degeneration. The increased collagen turnover rate and dysregulation may be the result of disrupted homeostasis where the IVD might be in a more catabolic state due to inflammation or other alterations to endogenous cellular homeostasis. Alternatively, it is also possible that the increased dysregulated turnover of collagen could represent the recurrent injury and repair process. These would potentially explain the increased levels of collagen degradation detected via CHP staining in DDD samples compared to the non-DDD control values.

Collagen plays an important role in mechanics of the AF.[49] Degeneration of collagen may impair the AF's ability to resist loads experienced by the IVD, and therefore, could be a central factor behind development of DDD. Degeneration is linked to reduced mechanical integrity of the AF.[50,51] There is a potential link between glycosaminoglycans and collagen which may govern the AF's structure–function relationship.[52] Future studies will explore the link(s) between collagen integrity and their role in mechanical changes observed during degeneration by using paired samples from non-DDD control donors and DDD surgical individuals.

The average mean fluorescence intensity and the average percentage of positively stained areal fraction with CHP decreased with age in non-DDD samples, which is contrary to the literature. Sivan and colleagues reported decreasing collagen turnover with increasing age in both non-DDD and DDD samples.[11,48] With decreasing collagen turnover, fewer binding sites for CHP on the collagen trimer may be exposed, which could lead to a decreased CHP signal as found in the current study. However, the opposite trend was determined for DDD samples where the CHP parameters increased with age. The CHP reagent may be binding to the exposed binding sites arising from the dysregulated collagen turnover processes and the dominating proteolytic processes associated with DDD.[53] Multiple studies have recognized the difficulty in differentiating physiological aging changes from disease-related changes.[54–56] This conundrum will require further studies to determine whether the two different processes differ mechanistically or share commonalities.

The histological degeneration score was increased for DDD samples compared to the non-DDD samples, indicating significant structural changes present in the DDD samples. However, there were weak to no correlations between the histological degeneration score and CHP parameters. This suggests that using histology alone as an assessment tool for collagen integrity may not capture some of the AF structural changes. In part, this could also relate to a lack of specificity of histological dyes towards degraded collagen molecules.

Increased mean fluorescence intensity (a measure of concentration of localized collagen degradation) and percent positive ROI area (a measure of spatial collagen integrity) represent two different, yet interconnected, methods to assess the integrity of the tissue collagen. Both parameters likely have a strong link, especially in the non-DDD samples. Three pathways of decreased collagen integrity are possible: (i) spatial changes in collagen integrity across the tissue occur first followed by local changes in collagen integrity based on fluorescence intensity at particular locations, (ii) local changes occur first, followed by the spatial changes, or (iii) both changes occur simultaneously. Based on the previous literature,[6,7] it is plausible that the structural changes start spatially, and then the process turns into a feedback loop of increasing local damage and spatial damage simultaneously. However, it is not possible to determine cause-and-effect relationship between spatial and local changes with the current data and due to the limitation of human studies being cross-sectional rather than longitudinal but may require appropriate future investigation.

In the current study, no statistical differences were observed between males and females in either condition. This finding goes against the sexual dimorphism of development of degenerative disc disease observed in the literature where females have been shown to have higher prevalence.[27] Mosley and colleagues also showed in murine models that females had a higher degeneration grade following an annular injury compared to males,[17] similar to the current study. However, the degeneration grade accounts for multiple disc components including AF, NP, and endplates. It is evident that the scoring system does not just consist of collagen structural information and could be the reason behind the differences in the findings. However, the SHG imaging parameters examining the collagen

organization in the same study were not determined to be different between males and females. Thus, it is likely that the higher prevalence of DDD among females may not be due to just structural differences in the collagen but could also include hormonal and mechanical differences affecting other components of the ECM.

Comparing the lumbar level differences between L4-L5 and L5-S1, trends (non-significant) suggest that the DDD L5-S1 samples may have decreased collagen integrity compared to the DDD L4-L5 samples whereas the non-DDD L4-L5 and L5-S1 samples had similar mean fluorescence intensity and percent positive ROI area. The trend could be due to the different mechanical environments of the two levels. The L5-S1 disc mostly undergoes axial compression with limited movement along other planes due to geometric constraints from the two sacroiliac joints and the connection of the iliolumbar ligaments to the ilium, providing greater stability to the L5-S1 disc.[32] The L4-L5 disc undergoes greater axial torsional and flexion/extension movement due to the presence of discs superiorly and inferiorly and doesn't have the same stability as the L5-S1 disc.[32] Furthermore, Teraguchi et al.[34] reported greater prevalence of disc degeneration for L5-S1 discs compared to L4-L5 discs in both men (47.3% vs. 34.2%) and women (56.3% vs. 49.4%) under 50 years old. However, the trend was reversed in the 50–59 years old age group where L4-L5 discs had greater prevalence of disc degeneration than L5-S1 discs for both men (74.5% vs. 50.8%) and women (73.9% vs. 70.4%). In the current study, 9 out of 13 DDD individuals were below 50 years old. Thus, as the discs degenerate, it is possible that the L5-S1 disc may have a greater probability of losing its stability and undergoing more structural defects than the L4-L5 disc upon degeneration.

The specificity of CHP towards denatured collagen of all subtypes differentiates it from other techniques that have been utilized in the past to assess collagen degradation such as SHG, LC-PolScope, anti-collagen antibodies, and histology. SHG and L-PolScope provide information regarding collagen disorganization but do not directly assess collagen integrity. The common approach has been to correlate the disorganization to collagen integrity, but this approach lacks accuracy for such an assessment. Anti-collagen antibodies are specific to only specific types of collagens and do not have the selectivity for all collagen types.[54] Histological stains do not provide any specificity towards denatured collagen, and thus they are likely not an appropriate tool for assessment of collagen integrity. The fluorescence of CHP can be measured, leading to direct quantification of collagen integrity. The CHP reagent employs a unique method of detection of collagen denaturation and one that no other method currently available can replicate to the same extent. It is evident that CHP can be used as an ex vivo tool to quantify the relative molecular collagen structural changes in AF tissue from surgical individuals with DDD.

The current study had limitations. First, the study was cross-sectional, with surgical individuals with advanced disease, and thus, no cause-and-effect conclusions can be made. Second, at the methodological level, mechanical damage from sectioning was not quantified and it may have reduced the relative differences between the groups. Furthermore, only three serial sections (one slide) per sample were stained with CHP instead of using multiple slides selected

systematically to investigate the damage profile throughout the tissue. Using multiple slides, each from a different tissue depth, would have helped quantify the complete damage profile. Third, no samples were collected from individuals with severely degenerated tissue as in many cases, insufficient tissue for testing was available for removal by the surgeons. Thus, sample selection bias was present in the DDD group, and the reported collagen damage may not reflect the full range of collagen damage occurring in individuals with very advanced disease. Despite this limitation, significant differences between non-DDD and DDD individuals were still detected. Fourth, samples were only selected from the anterior region of the IVD. The IVD is a heterogenous tissue, and the loading patterns and mechanical properties associated with collagen are location dependent. Thus, further sampling of different locations across the IVD could provide improved generalizability of the current findings. Lastly, CHP may not have been bound only to degraded collagen. Alternatively, collagen binding regions could have been exposed for interacting with CHP due to other molecules such as aggrecan and decorin being displaced from the collagen trimer.[57] As the collagen triple helix unwinds during turnover, it is difficult to distinguish whether CHP was binding specifically to only degraded collagen helix and requires future studies to examine this effect in more detail.

In the future, collagen integrity from CHP will be correlated with mechanical properties to better understand the structure–function relationship of the AF. This may provide further insights into the disease progression at both macro and micro scales. Further, CHP also carries the potential for in vivo imaging by combining it with fluorescent reagents used in clinical imaging. The data from the current study will be further expanded such that correlations with clinical parameters used for surgical decision-making may be established. These may help provide improved diagnosis, guide treatment plans, and monitor the outcomes for individuals with DDD or other spinal disorders.

5 | CONCLUSION

CHP is a tool that is reported to detect collagen degradation and changes in its integrity. However, the use of CHP in IVD has been limited in the literature given its novelty. The present study determined that the average mean fluorescence intensity and average area of the ROI positively stained with CHP were both increased among DDD samples compared to the non-DDD samples. The sex comparisons showed that males and females did not differ in structural changes to collagen at the molecular scale and the only differences were between the DDD and non-DDD sex subgroups. Although not statistically significant, trends showed L5-S1 discs may experience more structural degradation to the collagen compared to the L4-L5 disc. Based on linear regressions between the mean fluorescence intensity and percent positive ROI area, it is suggested that both parameters are strongly linked in both non-DDD and DDD groups, and it may provide further insights into the mechanism of collagen degradation. Overall, our results showed that the structural integrity of the collagen structure at the molecular scale is decreased among DDD individuals compared to that from non-DDD donors.

AUTHOR CONTRIBUTIONS

Study conceptualization and design: M.S.D., D.A.H., G.S., J.R.M., and N.A.D.; Data collection and experiments: M.S.D., D.P.; Data analysis: M.S.D.; Writing—Original draft: M.S.D.; Writing—Review and Editing: M.S.D., T.J.B., D.P., P.T.S., D.A.H., G.S., J.R.M., and N.A.D.

CONFLICT OF INTEREST STATEMENT

The authors declare no conflicts of interest.

ORCID

Manmeet S. Dhiman https://orcid.org/0009-0002-5386-8762
Ganesh Swamy https://orcid.org/0000-0002-3446-3105

REFERENCES

1. Ferreira ML, de Luca K, Haile LM, et al. Global, regional, and national burden of low back pain, 1990–2020, its attributable risk factors, and projections to 2050: a systematic analysis of the global burden of disease study 2021. *Lancet Rheumatol*. 2023;5(6):e316-e329. doi:10.1016/S2665-9913(23)00098-X
2. Adams MA. Biomechanics of back pain. *Acupunct Med J Br Med Acupunct Soc*. 2004;22(4):178-188. doi:10.1136/aim.22.4.178
3. Arnbak B, Jensen RK, Manniche C, et al. Identification of subgroups of inflammatory and degenerative MRI findings in the spine and sacroiliac joints: a latent class analysis of 1037 patients with persistent low back pain. *Arthritis Res Ther*. 2016;18(1):237. doi:10.1186/s13075-016-1131-x
4. Arnbak B, Jensen TS, Egund N, et al. Prevalence of degenerative and spondyloarthritis-related magnetic resonance imaging findings in the spine and sacroiliac joints in patients with persistent low back pain. *Eur Radiol*. 2016;26(4):1191-1203. doi:10.1007/s00330-015-3903-0
5. Luoma K, Vehmas T, Kerttula L, Grönblad M, Rinne E. Chronic low back pain in relation to Modic changes, bony endplate lesions, and disc degeneration in a prospective MRI study. *Eur Spine J*. 2016;25(9):2873-2881. doi:10.1007/s00586-016-4715-x
6. Vergroesen P-PA, Kingma I, Emanuel KS, et al. Mechanics and biology in intervertebral disc degeneration: a vicious circle. *Osteoarthr Cartil*. 2015;23(7):1057-1070. doi:10.1016/j.joca.2015.03.028
7. Adams MA, Roughley PJ. What is intervertebral disc degeneration, and what causes it? *Spine*. 2006;31(18):2151. doi:10.1097/01.brs.0000231761.73859.2c
8. Urban JP, Roberts S. Degeneration of the intervertebral disc. *Arthritis Res Ther*. 2003;5(3):120-130. doi:10.1186/ar629
9. Xiao L, Majumdar R, Dai J, et al. Molecular detection and assessment of intervertebral disc degeneration via a collagen hybridizing peptide. *ACS Biomater Sci Eng*. 2019;5(4):1661-1667. doi:10.1021/acsbiomaterials.9b00070

10. Feng H, Danfelter M, Strömqvist B, Heinegård D. Extracellular matrix in disc degeneration. *J Bone Joint Surg Am*. 2006;88(Suppl 2):25-29. doi:10.2106/JBJS.E.01341

11. Sivan SS, Hayes AJ, Wachtel E, et al. Biochemical composition and turnover of the extracellular matrix of the normal and degenerate intervertebral disc. *Eur Spine J*. 2014;23(3):344-353. doi:10.1007/s00586-013-2767-8

12. Li Y, Yu SM. Targeting and mimicking collagens via triple helical peptide assembly. *Curr. Opin. Chem. Biol.* 2013;17(6):968-975. doi:10.1016/j.cbpa.2013.10.018

13. Li Y, Ho D, Meng H, et al. Direct detection of collagenous proteins by fluorescently labeled collagen mimetic peptides. *Bioconjug Chem*. 2013;24(1):9-16. doi:10.1021/bc3005842

14. Hoy RC, D'Erminio DN, Krishnamoorthy D, et al. Advanced glycation end products cause RAGE-dependent annulus fibrosus collagen disruption and loss identified using in situ second harmonic generation imaging in mice intervertebral disk in vivo and in organ culture models. *Jor Spine*. 2020;3(4):e1126. doi:10.1002/jsp2.1126

15. Zeldin L, Mosley GE, Laudier D, et al. Spatial mapping of collagen content and structure in human intervertebral disk degeneration. *Jor Spine*. 2020;3(4):e1129. doi:10.1002/jsp2.1129

16. Ashinsky BG, Gullbrand SE, Bonnevie ED, et al. Multiscale and multimodal structure–function analysis of intervertebral disc degeneration in a rabbit model. *Osteoarthr Cartil*. 2019;27(12):1860-1869. doi:10.1016/j.joca.2019.07.016

17. Mosley GE, Hoy RC, Nasser P, et al. Sex differences in rat intervertebral disc structure and function following annular puncture injury. *Spine*. 2019;44(18):1257-1269. doi:10.1097/BRS.0000000000003055

18. Xiao L, Ding M, Fernandez A, Zhao P, Jin L, Li X. Curcumin alleviates lumbar radiculopathy by reducing neuroinflammation, oxidative stress and nociceptive factors. *Eur Cell Mater*. 2017;33:279-293. doi:10.22203/eCM.v033a21

19. Xiao L, Hong K, Roberson C, et al. Hydroxylated fullerene: a stellar Nanomedicine to treat lumbar Radiculopathy via antagonizing TNF-α-induced Ion Channel activation, calcium signaling, and neuropeptide production. *ACS Biomater Sci Eng*. 2018;4(1):266-277. doi:10.1021/acsbiomaterials.7b00735

20. Billinghurst RC, Buxton EM, Edwards MG, McGraw MS, McIlwraith CW. Use of an antineoepitope antibody for identification of type-II collagen degradation in equine articular cartilage. *Am J Vet Res*. 2001;62(7):1031-1039. doi:10.2460/ajvr.2001.62.1031

21. Zitnay JL, Li Y, Qin Z, et al. Molecular level detection and localization of mechanical damage in collagen enabled by collagen hybridizing peptides. *Nat Commun*. 2017;8(1):14913. doi:10.1038/ncomms14913

22. Zitnay JL, Jung GS, Lin AH, et al. Accumulation of collagen molecular unfolding is the mechanism of cyclic fatigue damage and failure in collagenous tissues. *Sci Adv*. 2020;6:eaba2795. doi:10.1126/sciadv.aba2795

23. Liu L, Huang K, Li W, et al. Molecular imaging of collagen destruction of the spine. *ACS Nano*. 2021;15(12):19138-19149. doi:10.1021/acsnano.1c07112

24. Seelemann CA, Willett TL. Empirical evidence that bone collagen molecules denature as a result of bone fracture. *J Mech Behav Biomed Mater*. 2022;131:105220. doi:10.1016/j.jmbbm.2022.105220

25. Gallate ZS, D'Erminio DN, Nasser P, Laudier DM, Iatridis JC. Galectin-3 and RAGE differentially control advanced glycation endproduct-induced collagen damage in murine intervertebral disc organ culture. *Jor Spine*. 2023;6(2):e1254. doi:10.1002/jsp2.1254

26. Bennink LL, Li Y, Kim B, et al. Visualizing collagen proteolysis by peptide hybridization: from 3D cell culture to in vivo imaging. *Biomaterials*. 2018;183:67-76. doi:10.1016/j.biomaterials.2018.08.039

27. Parenteau CS, Lau EC, Campbell IC, Courtney A. Prevalence of spine degeneration diagnosis by type, age, gender, and obesity using Medicare data. *Sci Rep*. 2021;11(1):5389. doi:10.1038/s41598-021-84724-6

28. de Schepper EIT, Damen J, van Meurs JBJ, et al. The association between lumbar disc degeneration and low back pain: the influence of age, gender, and individual radiographic features. *Spine*. 2010;35(5):531-536. doi:10.1097/BRS.0b013e3181aa5b33

29. Wang YXJ. Postmenopausal Chinese women show accelerated lumbar disc degeneration compared with Chinese men. *J Orthop Transl*. 2015;3(4):205-211. doi:10.1016/j.jot.2015.09.001

30. Wang Y-XJ, Griffith JF, Zeng XJ, et al. Prevalence and gender difference of lumbar disc space narrowing in elderly Chinese men and women: Mr. OS (Hong Kong) and Ms. OS (Hong Kong) studies. *Arthritis Rheum*. 2013;65(4):1004-1010. doi:10.1002/art.37857

31. Mosley GE, Wang M, Nasser P, et al. Males and females exhibit distinct relationships between intervertebral disc degeneration and pain in a rat model. *Sci Rep*. 2020;10:15120. doi:10.1038/s41598-020-72081-9

32. Okoro T, Sell P. A short report comparing outcomes between L4/L5 and L5/S1 single-level discectomy surgery. *J Spinal Disord Tech*. 2010;23(1):40-42. doi:10.1097/BSD.0b013e3181b38537

33. Sabnis AB, Chamoli U, Diwan AD. Is L5–S1 motion segment different from the rest? A radiographic kinematic assessment of 72 patients with chronic low back pain. *Eur Spine J*. 2018;27(5):1127-1135. doi:10.1007/s00586-017-5400-4

34. Teraguchi M, Yoshimura N, Hashizume H, et al. Prevalence and distribution of intervertebral disc degeneration over the entire spine in a population-based cohort: the Wakayama spine study. *Osteoarthr Cartil*. 2014;22(1):104-110. doi:10.1016/j.joca.2013.10.019

35. Wilke H-J, Rohlmann F, Neidlinger-Wilke C, Werner K, Claes L, Kettler A. Validity and interobserver agreement of a new radiographic grading system for intervertebral disc degeneration: part I. Lumbar spine. *Eur Spine J*. 2006;15(6):720-730. doi:10.1007/s00586-005-1029-9

36. Griffith JF, Wang YXJ, Antonio GE, et al. Modified Pfirrmann grading system for lumbar intervertebral disc degeneration. *Spine*. 2007;32(24):E708-E712. doi:10.1097/BRS.0b013e31815a59a0

37. le Maitre CL, Dahia CL, Giers M, et al. Development of a standardized histopathology scoring system for human intervertebral disc degeneration: an Orthopaedic Research Society spine section initiative. *Jor Spine*. 2021;4(2):e1167. doi:10.1002/jsp2.1167

38. Schneider CA, Rasband WS, Eliceiri KW. NIH image to ImageJ: 25 years of image analysis. *Nat Methods*. 2012;9(7):671-675. doi:10.1038/nmeth.2089

39. Mountain KM, Bjarnason TA, Dunn JF, Matyas JR. The functional microstructure of tendon collagen revealed by high-field MRI. *Magn Reson Med*. 2011;66(2):520-527. doi:10.1002/mrm.23036

40. Al-Saffar Y, Moo EK, Pingguan-Murphy B, Matyas J, Korhonen RK, Herzog W. Dependence of crack shape in loaded articular cartilage on the collagenous structure. *Connect Tissue Res*. 2023;64(3):294-306. doi:10.1080/03008207.2023.2166500

41. Haefeli M, Kalberer F, Saegesser D, Nerlich AG, Boos N, Paesold G. The course of macroscopic degeneration in the human lumbar intervertebral disc. *Spine*. 2006;31(14):1522. doi:10.1097/01.brs.0000222032.52336.8e

42. Roberts S, Evans H, Trivedi J, Menage J. Histology and pathology of the human intervertebral disc. *JBJS*. 2006;88(suppl_2):10-14. doi:10.2106/JBJS.F.00019

43. Ciapetti G, Granchi D, Devescovi V, et al. Ex vivo observation of human intervertebral disc tissue and cells isolated from degenerated intervertebral discs. *Eur Spine J*. 2012;21(1):10-19. doi:10.1007/s00586-012-2234-y

44. Hwang J, Huang Y, Burwell TJ, et al. *In situ* imaging of tissue remodeling with collagen hybridizing peptides. *ACS Nano*. 2017;11(10):9825-9835. doi:10.1021/acsnano.7b03150

45. Bonnans C, Chou J, Werb Z. Remodelling the extracellular matrix in development and disease. *Nat Rev Mol Cell Biol*. 2014;15(12):786-801. doi:10.1038/nrm3904

46. Wahyudi H, Reynolds AA, Li Y, Owen SC, Yu SM. Targeting collagen for diagnostic imaging and therapeutic delivery. *J Control Release*. 2016;240:323-331. doi:10.1016/j.jconrel.2016.01.007

47. Page-McCaw A, Ewald AJ, Werb Z. Matrix metalloproteinases and the regulation of tissue remodelling. *Nat Rev Mol Cell Biol*. 2007;8(3):221-233. doi:10.1038/nrm2125

48. Sivan S-S, Wachtel E, Tsitron E, et al. Collagen turnover in Normal and degenerate human intervertebral discs as determined by the racemization of aspartic acid*. *J Biol Chem*. 2008;283(14):8796-8801. doi:10.1074/jbc.M709885200

49. Isaacs JL, Vresilovic E, Sarkar S, Marcolongo M. Role of biomolecules on annulus fibrosus micromechanics: effect of enzymatic digestion on elastic and failure properties. *J Mech Behav Biomed Mater*. 2014;40:75-84. doi:10.1016/j.jmbbm.2014.08.012

50. Acaroglu ER, Iatridis JC, Setton LA, Foster RJ, Mow VC, Weidenbaum M. Degeneration and aging affect the tensile behavior of human lumbar anulus fibrosus. *Spine*. 1995;20(24):2690-2701. doi:10.1097/00007632-199512150-00010

51. Fujita Y, Duncan NA, Lotz JC. Radial tensile properties of the lumbar annulus fibrosus are site and degeneration dependent. *J Orthop Res*. 1997;15(6):814-819. doi:10.1002/jor.1100150605

52. Jacobs NT, Smith LJ, Han WM, Morelli J, Yoder JH, Elliott DM. Effect of orientation and targeted extracellular matrix degradation on the shear mechanical properties of the annulus fibrosus. *J Mech Behav Biomed Mater*. 2011;4(8):1611-1619. doi:10.1016/j.jmbbm.2011.03.016

53. Weiler C, Nerlich A, Zipperer J, Bachmeier B, Boos N. 2002 SSE award competition in basic science: expression of major matrix metalloproteinases is associated with intervertebral disc degradation and resorption. *Eur Spine J*. 2002;11(4):308-320. doi:10.1007/s00586-002-0472-0

54. Antoniou J, Steffen T, Nelson F, et al. The human lumbar intervertebral disc: evidence for changes in the biosynthesis and denaturation of the extracellular matrix with growth, maturation, ageing, and degeneration. *J Clin Invest*. 1996;98(4):996-1003.

55. Adams MA, Dolan P. Intervertebral disc degeneration: evidence for two distinct phenotypes. *J Anat*. 2012;221(6):497-506. doi:10.1111/j.1469-7580.2012.01551.x

56. Wu Q, Huang JH. Intervertebral disc aging, degeneration, and associated potential molecular mechanisms. *J Head Neck Spine Surg*. 2017;1(4):555569. doi:10.19080/JHNSS.2017.01.555569

57. Han B, Li Q, Wang C, et al. Decorin regulates the Aggrecan network integrity and biomechanical functions of cartilage extracellular matrix. *ACS Nano*. 2019;13(10):11320-11333. doi:10.1021/acsnano.9b04477

SUPPORTING INFORMATION

Additional supporting information can be found online in the Supporting Information section at the end of this article.